

# Energy Gaps and Stark Effect in Boron Nitride Nanoribbons

Cheol-Hwan Park and Steven G. Louie\*

Department of Physics, University of California at Berkeley,  
Berkeley, California 94720

Received March 9, 2008; Revised Manuscript Received May 7, 2008

## ABSTRACT

A first-principles investigation of the electronic properties of boron nitride nanoribbons (BNNRs) having either armchair or zigzag shaped edges passivated by hydrogen with widths up to 10 nm is presented. Band gaps of armchair BNNRs exhibit family dependent oscillations as the width increases and, for ribbons wider than 3 nm, converge to a constant value that is 0.02 eV smaller than the bulk band gap of a boron nitride sheet owing to the existence of very weak edge states. The band gap of zigzag BNNRs monotonically decreases and converges to a gap that is 0.7 eV smaller than the bulk gap due to the presence of strong edge states. When a transverse electric field is applied, the band gaps of armchair BNNRs decrease monotonically with the field strength. For the zigzag BNNRs, however, the band gaps and the carrier effective masses either increase or decrease depending on the direction and the strength of the field.

Two-dimensional crystals, including graphene and single layer of hexagonal boron nitride (BN), have recently been fabricated.<sup>1</sup> Among them, only graphene has been studied extensively.<sup>2</sup> Unlike graphene, a hexagonal BN sheet is a wide gap insulator like bulk hexagonal BN<sup>3</sup> and is a promising material in optics and opto-electronics.<sup>4</sup>

Graphene nanoribbons (GNRs)<sup>5</sup> with width a few to a hundred nanometers have been produced by lithographical patterning<sup>6,7</sup> or chemical processing<sup>8</sup> of graphene. We expect that boron nitride nanoribbons (BNNRs) could also be made using similar or other techniques. Figure 1a,b shows the structures of an armchair BNNR with  $N_a$  dimer lines ( $N_a$ -aBNNR) and a zigzag BNNR with  $N_z$  zigzag chains ( $N_z$ -zBNNR), respectively. A tight-binding study of the band-structures of 21-aBNNR and 13-zBNNR (corresponding to widths  $\sim 3$  nm)<sup>9</sup> and first-principles investigations of the electronic properties of small width BNNRs<sup>10,11</sup> have been reported. However, to our knowledge, first-principles calculations on the electronic properties of experimentally realizable size of BNNRs have not been performed.

Under a transverse electric field, carbon nanotubes with impurity atoms are expected to show novel band gap opening behaviors,<sup>12</sup> whereas zigzag GNRs reveal half-metallicity.<sup>13</sup> On the other hand, single-walled boron nitride nanotubes (SW-BNNTs), which are rolled up BN sheets,<sup>14,16</sup> have been predicted to show gigantic Stark effect in their band gaps in response to a transverse electric field,<sup>17</sup> and this effect has been confirmed experimentally.<sup>18</sup> The effect becomes stronger in larger diameter SW-BNNTs.<sup>17</sup> A similar phenomenon is expected in BNNRs. Unlike SW-BNNTs, however,

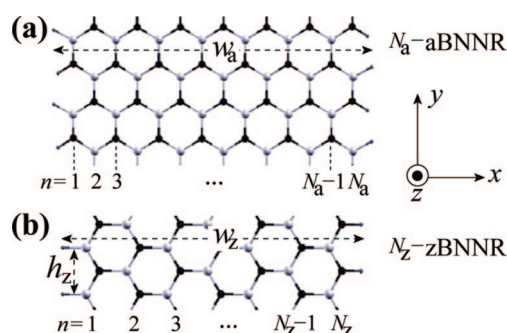


**Figure 1.** Schematic of (a) 14-aBNNR and (b) 7-zBNNR passivated by hydrogen atoms. Boron, nitrogen, and hydrogen atoms are represented by white, black, and gray spheres, respectively. BNNRs are periodic along the  $y$  direction.

BNNRs can be arbitrarily wide. Therefore, the consequences of the Stark effect in BNNRs would be even more dramatic than in SW-BNNTs.

In this study, we report first-principles calculations on the electronic properties of armchair and zigzag BNNRs up to width of 10 nm with hydrogen passivation of the edge carbon atoms. We show that the band gaps of armchair and zigzag BNNRs do not converge to the same value even when the ribbons are very wide. The band gap of armchair BNNRs, obtained by density functional theory (DFT) calculations within the local density approximation (LDA), converges to a value that is 0.02 eV smaller than the LDA band gap of 4.53 eV of a BN sheet.<sup>19</sup> Unlike armchair GNRs, the lowest unoccupied band of the armchair BNNRs is composed of edge states with energy position asymptote to a fixed value when the ribbon is wider than 3 nm, the decay length of the

\* Corresponding author. E-mail: sglouie@berkeley.edu.

edge-state. The band gap of the zigzag BNNRs, also determined by edge states, is monotonically reduced as a function of increasing width and converges to a value that is 0.7 eV smaller than the LDA bulk gap because, as discussed below, of an additional edge polarization charge effect. The DFT Kohn–Sham eigenvalues within LDA in general underestimate the band gaps of materials; an accurate first-principles calculation of band gaps requires a quasi-particle approach.<sup>20</sup> The basic physics discovered here however should not be changed.

When a transverse electric field is applied, the highest occupied and the lowest empty states in armchair BNNRs become localized at the two different edges. Because of the external electrostatic potential difference between the two edges, the band gap is reduced with increased field strength. On the contrary, in zigzag BNNRs, depending on the field direction, the states near the band gap either become more localized at the edges or less so. Also, the band gaps and effective masses either decrease or increase depending on field strength and direction. These novel properties could be used in manipulating the transport properties of doped BNNRs.

We performed ab initio pseudopotential DFT calculations within LDA in a supercell configuration using the SIESTA computer code.<sup>21</sup> A double- $\zeta$  plus polarization basis set was used, and ghost orbitals were included to describe free-electron-like states.<sup>3,17,22</sup> A charge density cutoff of 300 Ry was used, and atomic positions were relaxed so that the force on each atom is less than 0.04 eV/Å. To eliminate spurious interactions between periodic images, a supercell size of up to 20 nm  $\times$  20 nm in the  $xz$  plane was used.

The armchair BNNRs are found to have a direct gap at the zone center (left panel of Figure 2a). The highest occupied state, the valence band maximum (VBM), has a wave function which is localized at nitrogen atoms throughout the ribbon (right lower panel of Figure 2a). The lowest empty state, the conduction band minimum (CBM), is however an edge state with wave function localizing at the boron atoms on the edges (right upper panel of Figure 2a). In contrast, the corresponding state for an armchair GNRs is delocalized throughout the ribbon.<sup>23</sup> The total potential near the edge of the armchair BNNRs is different from that of the bulk.<sup>24</sup> By incorporating this variation into the on-site potential energies of a few BN dimer lines near the edges, one could reproduce the main features of the states near the band gap within a tight-binding formulation.<sup>24</sup>

The zigzag BNNRs have the VBM at a point between the X and the  $\Gamma$  points which has wave function localized at the nitrogen edge and have the CBM at the X point which has wave function localized at the boron edge (Figure 3a), in agreement with results by Nakamura et al.<sup>10</sup>

Figure 4a shows the band gap variation of the armchair and the zigzag BNNRs with width. The most interesting and somewhat counter-intuitive feature is that, as the width increases, band gaps of the armchair and the zigzag BNNRs converge to different values neither of which are that of a BN sheet. This is because the CBM or the VBM are determined by edge states.

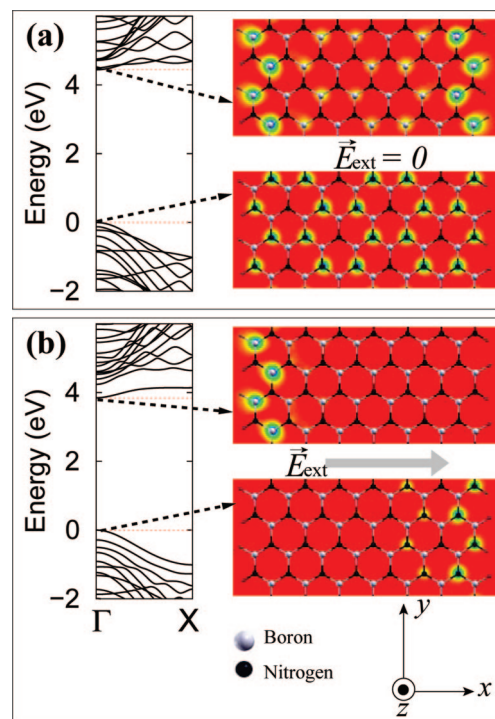


**Figure 2.** LDA energy bandstructure (left) and the squared wave functions integrated along  $z$  of the highest occupied state (right lower) and the lowest unoccupied state (right upper) of 14-aBNNR under an external electric field  $\vec{E}_{ext}$  of strength (a) zero and (b) 0.1 eV/Å along  $+x$  direction. Dashed red lines in the bandstructure indicate the energies of the band edge states. In the wave function plots, green regions are associated with high densities.

The edge-state band gaps of armchair BNNRs show a family behavior with respect to the number of dimer lines  $N_a$  (inset of Figure 4a), the family with  $N_a = 3n - 1$  having the smallest gaps where  $n$  is an integer. A similar trend is observed in armchair GNRs.<sup>23,25,28</sup> The edge-state band gaps of the armchair BNNRs converge to a near constant value roughly when the ribbon is wider than 3 nm (Figure 4a). This characteristic length is related to the decay length of the CBM edge state. Figure 4b shows the squared electron wave functions of the CBM states of 14-aBNNR and 26-aBNNR integrated in the  $yz$  plane. These states are localized on the boron atoms near the two edges. When the width is about 3 nm as in the 26-aBNNR, the wave function from the two edges begins to decouple and thus stabilizing its energy position.

In zigzag BNNRs, the boron edge and the nitrogen edge are negatively and positively charged (electronic plus ionic charge), respectively. Because of this polarization, the potential felt by electrons is higher at the boron edge and lower at the nitrogen edge, contributing a factor which increases the band gap of the narrow zBNNRs since the VBM and the CBM are edge states localized at the nitrogen edge and the boron edge, respectively (Figure 3a). However, as the ribbon becomes wider, the effective polarization line charge density  $\sigma_{eff}$ , defined as

$$\sigma_{eff} \equiv \hat{n} \times \frac{1}{w_z h_z} \int_{r \in \text{unit cell}} d\mathbf{r} \rho(\mathbf{r})$$

where  $\rho(\mathbf{r})$  is the total charge density including the core

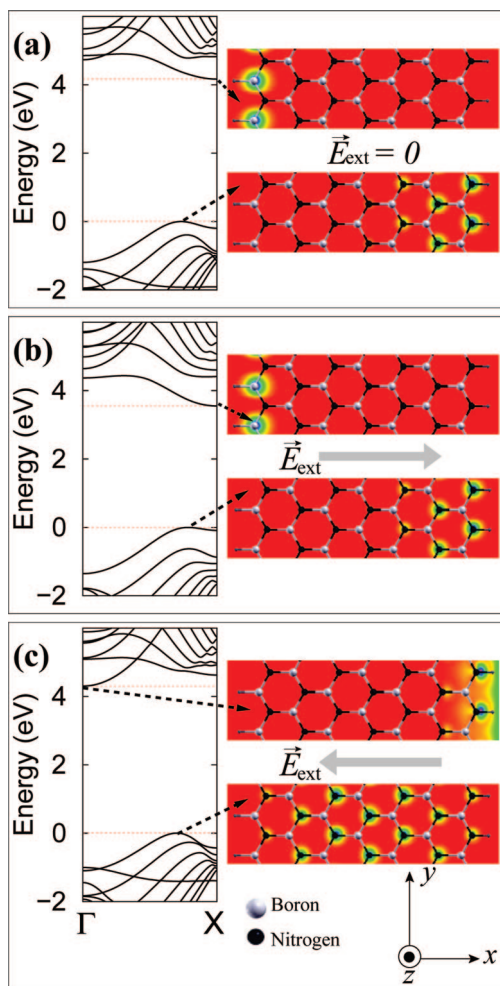


**Figure 3.** LDA energy bandstructure (left) and the squared wave functions integrated along  $z$  of the highest occupied state (right lower) and the lowest unoccupied state (right upper) of 7-zBNNR under an external electric field  $\vec{E}_{ext}$  of strength (a) zero, (b) 0.1 eV/Å and (c) -0.1 eV/Å along the  $x$  direction. Dashed red lines in the bandstructure indicate the energies of the band edge states. In the wave function plots, green regions are associated with high densities.

charge, and  $h_z$  is the spatial period along the  $y$  direction (see Figure 1b), decreases as  $\sim 1/w_z$  (Figure 4c) because of an increased screening, resulting in the decrease and convergence of the band gap as  $w_z$  increases.

Figure 2b shows how the bandstructure and wave functions of a 14-aBNNR change under a 0.1 eV/Å transverse electric field. Owing to the Stark effect, the wave functions of the highest occupied and the lowest unoccupied states now localize at the opposite edges where the external electrostatic potential felt by an electron is higher and lower, respectively (right panel of Figure 2b). Thus, the band gaps of armchair BNNRs decrease when a transverse electric field is applied (left panel of Figure 2b). A similar behavior has been predicted<sup>17</sup> and observed<sup>18</sup> in BNNTs.

Figure 3b,c shows how the bandstructure and the edge-state wave functions of a 7-zBNNR change under a 0.1 eV/Å transverse electric field. When an electric field is applied toward  $+x$  direction, the VBM and CBM edge-state wave functions do not change qualitatively (right panel of Figure 3b). Thus, for a similar reason as in the armchair BNNRs,

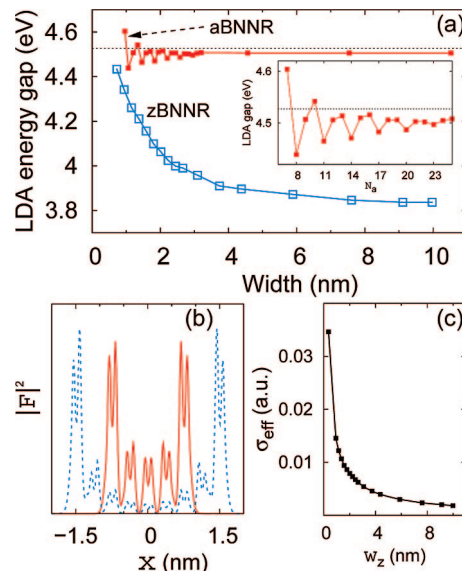


**Figure 4.** (a) Band gaps of armchair (filled red squares) and zigzag (empty blue squares) BNNRs versus their widths. Inset: band gaps of armchair BNNRs versus  $N_a$  (see Figure 1). Solid lines are a guide to the eyes. Dashed lines indicate the bulk band gap of a BN sheet with no edges. (b) Probability distributions  $|\Phi(r)|^2$  integrated in the  $yz$  plane (see Figure 1) versus the distance along the  $x$  direction from the ribbon center for the lowest unoccupied state in 14-aBNNR (solid red line) and 26-aBNNR (dashed blue line). (c) The effective polarized line charge density  $\sigma_{eff}$  of zigzag BNNRs versus  $w_z$ . The solid line is a guide to the eyes.

the band gap decreases (left panel of Figure 3b). When the electric field is applied along the  $-x$  direction, the potential felt by an electron localized at the right edge (the nitrogen edge) is decreased whereas that at the left edge (the boron edge) is increased. Therefore, the energy gap between these two states increases as shown in Figure 3c. (Actually, the energy of the original lowest empty state has been pushed upward by so much that the state is no longer the CBM state.) At the same time, the VBM states tend to delocalize (right lower panel of Figure 3c).

Figure 5a,b shows the band gap variation of BNNRs with field strength. In armchair BNNRs, the band gap decreases when the field strength increases regardless of its direction (Figure 5a). A similar behavior has been observed in SW-BNNTs.<sup>17</sup> For example, for the 10 nm wide 84-aBNNR the LDA band gap is reduced from 4.5 eV to less than 1.0 eV under a 0.1 eV/Å field. In zigzag BNNRs, at small field strength, the band gap decreases when the field is along  $+x$  direction but increases when the field is reversed (Figure 5b). In other words, zigzag BNNRs show asymmetric Stark effect. However, as the field becomes stronger, the band gap decreases regardless of the direction. Moreover, the band gap variations, when plotted against the difference in the external electrostatic potential between the two edges, fall on a universal curve for ribbons with different widths (insets of Figure 5a,b). This is because the gap determining states localize on different edges as the field becomes strong; thus, the change in their energy difference is directly related to the potential difference between the edges.

Figure 5c,d shows the effective mass of the hole carrier at the VBM for a range of external field strength. In armchair



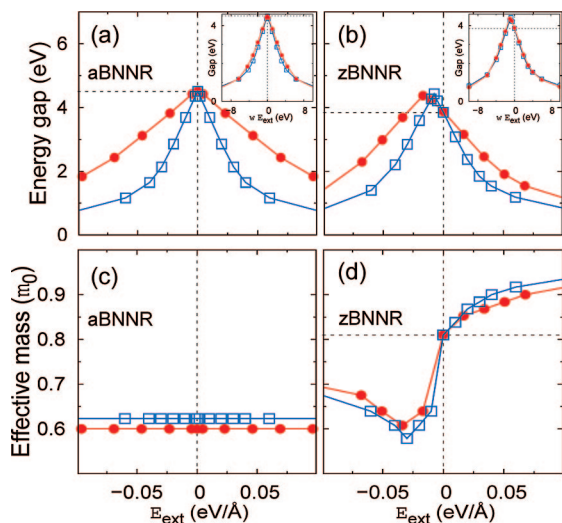


**Figure 5.** (a,c) LDA energy gaps and effective hole masses (in units of the free electron mass  $m_0$ ) of the highest occupied band in 36-aBNNR (filled red circles) and 84-aBNNR (empty blue squares) under a transverse electric field versus the field strength. The inset in (a) shows energy gaps as a function of the external potential difference between the two edges. (b,d) Similar quantities as in (a) and (c) for 27-zBNNR (filled red circles) and 46-zBNNR (empty blue squares), respectively.

BNNRs, the hole mass of the VBM is independent of the field strength. In contrast, the corresponding effective mass in zigzag BNNRs changes with the external field, and even more interestingly, in an asymmetric way. In particular, when the field is along the  $-x$  direction, the effective mass decreases substantially. Within  $\pm 0.02$  eV/Å variation of the field, the effective mass can be varied by 50% from  $0.6m_0$  to  $0.9m_0$  where  $m_0$  is the free electron mass. In the case of electron carriers in zigzag BNNRs, a nearly free-electron state<sup>3,17,22</sup> becomes the CBM if a field stronger than a critical value, depending on the width, is applied (see Figure 3c) and the characteristics of charge carriers change significantly. These novel phenomena demonstrate the possibility of tuning carrier mobilities of doped BNNRs by applying a transverse electric field.

In summary, we have studied the electronic properties of BNNRs as a function of width with or without external transverse electric fields. The band gap of the armchair BNNR and that of the zigzag BNNR are determined by edge states and thus converge to values different from that of the bulk BN sheet. The electronic and the transport properties of BNNRs are shown to be tunable by an external transverse electric field. Especially, zigzag BNNRs are shown to exhibit asymmetric response to the electric field.

Additional remark: After completion of the work and during the preparation of this manuscript, we became aware of a related work on similar systems from another group.<sup>29</sup>

**Acknowledgment.** We thank A. Khoo, J. D. Sau, E. Kioupakis, and F. Giustino for fruitful discussions and Y.-W. Son for a critical reading of the manuscript. This work was supported by NSF Grant DMR07-05941 and by the Director, Office of Science, Office of Basic Energy Sciences, Division of Materials Sciences and Engineering Division, U.S. Department of Energy under Contract No. DE-AC02-05CH11231. Computational resources have been provided by NPACI and NERSC.

## References

- (1) Novoselov, K. S.; Jiang, D.; Schedin, F.; Booth, T.; Khotkevich, V. V.; Morozov, S. V.; Geim, A. K. *Proc. Natl. Acad. Sci. U.S.A.* **2005**, *102*, 10451–10453.
- (2) Geim, A. K.; Novoselov, K. S. *Nat. Mater.* **2007**, *6*, 183–191.
- (3) Blase, X.; Rubio, A.; Louie, S. G.; Cohen, M. L. *Phys. Rev. B* **1995**, *51*, 6868–6875.
- (4) Watanabe, K.; Taniguchi, T.; Kanda, H. *Nat. Mater.* **2004**, *3*, 404–409.
- (5) Nakada, K.; Fujita, M.; Dresselhaus, G.; Dresselhaus, M. S. *Phys. Rev. B* **1996**, *54*, 17954–17961.
- (6) Han, M. Y.; Özyilmaz, B.; Zhang, Y.; Kim, P. *Phys. Rev. Lett.* **2007**, *98*, 206805.
- (7) Chen, Z.; Lin, Y.-M.; Rooks, M. J.; Avouris, P. *Physica E* **2007**, *40*, 228.
- (8) Li, X.; Wang, X.; Zhang, L.; Lee, S.; Dai, H. *Science* **2008**, *319*, 1229–1232.
- (9) Chen, R. B.; Chang, C. P.; Shyu, F. L.; Lin, M. F. *Solid State Commun.* **2002**, *123*, 365–369.
- (10) Nakamura, J.; Nitta, T.; Natori, A. *Phys. Rev. B* **2005**, *72*, 205429.
- (11) Du, A.; Smith, S. C.; Lu, G. *Chem. Phys. Lett.* **2007**, *447*, 181.
- (12) Son, Y.-W.; Ihm, J.; Cohen, M. L.; Louie, S. G.; Choi, H. J. *Phys. Rev. Lett.* **2005**, *95*, 216602.
- (13) Son, Y.-W.; Cohen, M. L.; Louie, S. G. *Nature* **2006**, *444*, 347–349.
- (14) Rubio, A.; Corkill, J. L.; Cohen, M. L. *Phys. Rev. B* **1994**, *49*, 5081–5084.
- (15) Blase, X.; Rubio, A.; Louie, S. G.; Cohen, M. L. *Europhys. Lett.* **1994**, *28*, 335–340.
- (16) Chopra, N.; Luyken, J.; Cherry, K.; Crespi, V. H.; Cohen, M. L.; Louie, S. G.; Zettl, A. *Science* **1995**, *269*, 966–967.
- (17) Khoo, K. H.; Mazzoni, M. S. C.; Louie, S. G. *Phys. Rev. B* **2004**, *69*, 201401.
- (18) Ishigami, M.; Sau, J. D.; Aloni, S.; Cohen, M. L.; Zettl, A. *Phys. Rev. Lett.* **2005**, *94*, 056804.
- (19) In this paper, we define the bulk gap as the electronic energy band gap of an infinitely extended boron nitride sheet without edges.
- (20) Hybertsen, M. S.; Louie, S. G. *Phys. Rev. B* **1986**, *34*, 5390–5413.
- (21) Portal, D.; Artacho, O.; Ordejon, P.; Artacho, E.; Soler, J. *Int. J. Quantum Chem.* **1997**, *65*, 453–461.
- (22) Park, C.-H.; Spataru, C. D.; Louie, S. G. *Phys. Rev. Lett.* **2006**, *96*, 126105.
- (23) Brey, L.; Fertig, H. A. *Phys. Rev. B* **2006**, *73*, 235411.
- (24) Park, C.-H.; Louie, S. G., unpublished.
- (25) Fujita, M.; Wakabayashi, K.; Nakada, K.; Kusakabe, K. *J. Phys. Soc. Jpn.* **1996**, *65*, 1920–1923.
- (26) Son, Y.-W.; Cohen, M. L.; Louie, S. G. *Phys. Rev. Lett.* **2006**, *97*, 216803.
- (27) Barone, V.; Hod, O.; Scuseria, G. E. *Nano Lett.* **2006**, *6*, 2748–2754.
- (28) White, C. T.; Li, J.; Gunlycke, D.; Mintmire, J. W. *Nano Lett.* **2007**, *7*, 825–830.
- (29) Zhang, Z.; Guo, W. *Phys. Rev. B* **2008**, *77*, 075403.

NL080695I